



## Original Research

# The PER1/HIF-1alpha negative feedback loop promotes ferroptosis and inhibits tumor progression in oral squamous cell carcinoma

Yixin Yang<sup>a</sup>, Hong Tang<sup>a</sup>, Jiawen Zheng<sup>a</sup>, Kai Yang<sup>a,\*</sup>

<sup>a</sup> Department of Oral and Maxillofacial Surgery, The First Affiliated Hospital of Chongqing Medical University, No.1, Youyi Road, Yuzhong District, Chongqing 400016, China



## ARTICLE INFO

## Keywords:

Ferroptosis  
Oral cancer  
Period 1  
HIF-1alpha  
Clock genes

## ABSTRACT

Current studies have proven that the decreased expression of the core circadian clock gene Period 1 (PER1) is closely related to the occurrence and progression of multiple malignant tumors, including oral squamous cell carcinoma (OSCC). But the mechanism involved is largely unknown. In this study, we found that PER1 was negatively correlated with the expression of the key ferroptosis-regulated proteins glutathione peroxidase (GPX4) and hypoxia inducible factor-1alpha (HIF-1α) in OSCC tissues. The expression of the ferroptosis related proteins GPX4, solute carrier family 7 member 11 (SLC7A11) and transferrin receptor (TFRC) and the levels of glutathione (GSH), malondialdehyde (MDA), reactive oxygen species (ROS) and Fe<sup>2+</sup> were detected in OSCC cells with overexpression or silencing of *PER1*. Mitochondrial morphology changes were observed. We found that PER1 promotes ferroptosis depending on HIF-1α in OSCC cells. *In vivo* tumorigenicity assays proved that PER1 overexpression inhibits HIF-1α, promotes ferroptosis and suppresses OSCC growth. Mechanistically, coimmunoprecipitation and cycloheximide tracking assays proved that PER1 binds to HIF-1α to promote HIF-1α protein degradation. ChIP and dual luciferase reporter assays proved that HIF-1α binds to the *PER1* promoter leading to feedback inhibition of *PER1* transcription. Our findings suggest that targeting the PER1/HIF-1α negative feedback loop may provide a new strategy for OSCC treatment.

## List of abbreviations

ANT	adjacent non-cancerous tissues
ChIP	chromatin immunoprecipitation assay
CHX	cycloheximide
Co-IP	coimmunoprecipitation
GPX4	glutathione peroxidase
GSH	glutathione
HIF-1α	hypoxia inducible factor-1alpha
HRP	horseradish peroxidase
IHC	immunohistochemistry
LPO	lipid peroxidation
MDA	malondialdehyde
OSCC	oral squamous cell carcinoma
PER1	period 1
ROS	reactive oxygen species
SLC7A11	solute Carrier Family 7 Member 11
TEM	transmission electron microscope
TFRC	transferrin Receptor

## Introduction

Oral cancer is one of the most common head and neck cancers [1, 2]. There are more than 370,000 new cases of oral cancer every year worldwide, and approximately 170,000 deaths from oral cancer every year [2]. Oral squamous cell carcinoma (OSCC) accounts for approximately 90% of oral cancers [3]. Although the current surgical techniques, radiotherapy and chemotherapy have made great progress, the mortality rate of oral cancer has increased at a rate of 0.5% per year [4]. In the past 30 years, the overall survival rate of patients with oral squamous cell carcinoma has been maintained at approximately 50% without significant improvement [5, 6]. Therefore, an in-depth study of the molecular mechanism of the initiation and progression of OSCC is needed to develop new and effective treatment methods.

Circadian clock genes exist in almost all cells of the human body [7, 8], and participate in the regulation of various important biochemical and physiological processes in organisms [9, 10]. The abnormal expression of these genes is an important factor in the occurrence of multiple diseases, including cancer [11, 12]. *PER1* is one of the core

\* Corresponding author.

E-mail address: [cqfyk@hotmail.com](mailto:cqfyk@hotmail.com) (K. Yang).

<https://doi.org/10.1016/j.tranon.2022.101360>

Received 24 January 2022; Accepted 25 January 2022

Available online 5 February 2022

1936-5233/© 2022 The Authors.

Published by Elsevier Inc.

This is an open access article under the CC BY-NC-ND license

(<http://creativecommons.org/licenses/by-nc-nd/4.0/>).

circadian clock genes [7–10]. Current studies have shown that disordered PER1 expression is closely related to the occurrence and progression of various cancers such as non-small cell lung cancer and gastric cancer [13–16]. We previously found that PER1 expression was reduced in OSCC tissues, and was significantly related to the TNM staging and poor prognosis of patients [17, 18]. The studies above show the importance of PER1 in anticancer effects, but the specific mechanism is still unclear. A deeper study of the mechanism may lead to valuable discoveries.

Ferroptosis is a new mode of cell death that has been discovered in recent years [19], and its main feature is that excess accumulation of iron-dependent lipid peroxides leads to cell death [20]. Current studies have shown that ferroptosis plays an important role in the occurrence and progression of multiple cancers including OSCC [21–24]. As ferroptosis is different from the cell death modes of necrosis, apoptosis and autophagy [19, 20], an in-depth study of the regulatory mechanism of ferroptosis may help to discover new strategies for cancer treatment. However, whether PER1 can regulate ferroptosis in cancer cells is currently unclear. Current research has proven that hypoxia inducible factor-1 $\alpha$  (HIF-1 $\alpha$ ) is one of the key proteins regulating ferroptosis [25–27]. Both the PER1 and HIF-1 $\alpha$  proteins contain the PER-ARNT-SIM (PAS) domain [28], and proteins often bind to each other through this domain [28, 29]. Chilov, D., et al. reported that the PER1 and HIF-1 $\alpha$  proteins can bind to each other in mouse brain tissue [30], but the functional effect of this combination is still unclear. Here we speculate that PER1 may affect the initiation and development of cancer by binding to HIF-1 $\alpha$  to regulate ferroptosis.

In this study, the results showed for the first time that PER1 inhibits OSCC growth by promoting ferroptosis *in vitro* and *in vivo*. We showed that the PER1 protein binds to the HIF-1 $\alpha$  protein and promotes HIF-1 $\alpha$  protein degradation, while HIF-1 $\alpha$  binds to the *PER1* promoter to inhibit *PER1* transcription in OSCC cells. These results suggest that the binding of PER1 and HIF-1 $\alpha$  forms a PER1/HIF-1 $\alpha$  negative feedback loop to amplify the effect of PER1 on regulating ferroptosis in cancer cells. In summary, our findings suggest that targeting the PER1/HIF-1 $\alpha$  negative feedback loop may be a promising therapeutic approach for the inhibiting the initiation and progression of OSCC.

## Materials and methods

The details of all relevant Materials and Methods below can be found in The Supplementary Materials and Methods

### Cell culture

Human oral mucosal HOK cells, and oral squamous cell carcinoma cell line TSCCA, SCC15 and CAL27 were culture routinely.

### Clinical specimens

Paraffin-embedded tissue sections of OSCC patients were obtained from the Department of Pathology, the First Affiliated Hospital of Chongqing Medical University. This study was approved by the Biomedical Ethics Committee of the First Affiliated Hospital of Chongqing Medical University (approval number: 2016–124). Informed consent was obtained from all patients.

### Vector construction

The plasmids were designed and synthesized by GeneChem (Shanghai, China). The sequence of shRNA is provided in Supplementary Table 1. The primers of cDNA are provided in Supplementary Table 2.

### Construction of stable transfected cells

TSCCA cells with stable PER1 silencing (sh-PER1-TSCCA) and SCC15 and CAL27 cells with stable PER1 overexpression (OE-PER1-SCC15 and OE-PER1-CAL27) were harvested. Negative control of TSCCA cells (NC-TSCCA), SCC15 (vector-SCC15) cells and CAL27 cells (vector-CAL27) were harvested.

### Immunohistochemistry (IHC)

Immunohistochemistry was carried out according to the instructions of the immunohistochemistry detection kit (Beijing, Zhongshan Jinqiao, SP-9000). The antibody information is available in Supplementary Table 3. The result was evaluated by the dual score semiquantitative method (Allred score) [31].

### RT-qPCR

The primer sequences of PER1, HIF-1 $\alpha$  and the internal reference gene  $\beta$ -actin are shown in Supplementary Table 4. The mRNA expression of each gene was calculated using the  $2^{-\Delta\Delta Ct}$  method.

### Western blotting

Cells were lysed with RIPA lysis buffer (P0013B, Beyotime, Shanghai, China) containing PMSF. A BCA protein quantification kit (P0010, Beyotime) was used to determine the protein concentration. Proteins were separated by SDS-PAGE and transferred to a PVDF membrane. The details of the antibodies used in Western blotting are shown in Supplementary Table 3.

### Detection of malondialdehyde (MDA) concentration

MDA levels were detected using an MDA detection kit (BC0025, Solarbio) according to the instructions. MDA level (nmol/mgProt) =  $5 \times 12.9 \times (\Delta A_{532} \times \Delta A_{600} - 2.58 \times \Delta A_{450}) / \text{Cpr}$ .

### Measurement of glutathione (GSH) content

GSH levels were detected with a micro reduced glutathione determination kit (A006–2–1, Nanjing Jiancheng) according to the instructions. GSH content ( $\mu\text{mol/gprot}$ ) = (measured OD value-blank OD value) / (standard OD value-blank OD value)  $\times$  (20  $\mu\text{mol/L}$ )  $\times$  2/protein concentration (gProt/L).

### Measurement of ROS content

ROS levels were detected using a reactive oxygen detection kit (S0033S, Beyotime) according to the instructions.

### Detection of the intracellular Fe<sup>2+</sup> level

FerroOrange (F-374, Dojindo) was used to detect the intracellular Fe<sup>2+</sup> level. Three fluorescence images were photographed in randomly selected fields using fluorescence microscopy (BX51TRF, OLYMPUS, Japan) under the same exposure conditions. ImageJ software was used to calculate the fluorescence positive rate.

### Transmission electron microscope (TEM) assay

Cell morphology was observed, and photos were taken using a transmission electron microscope.

### Coimmunoprecipitation (co-IP)

The cell lysates were immunoprecipitated with protein A/G

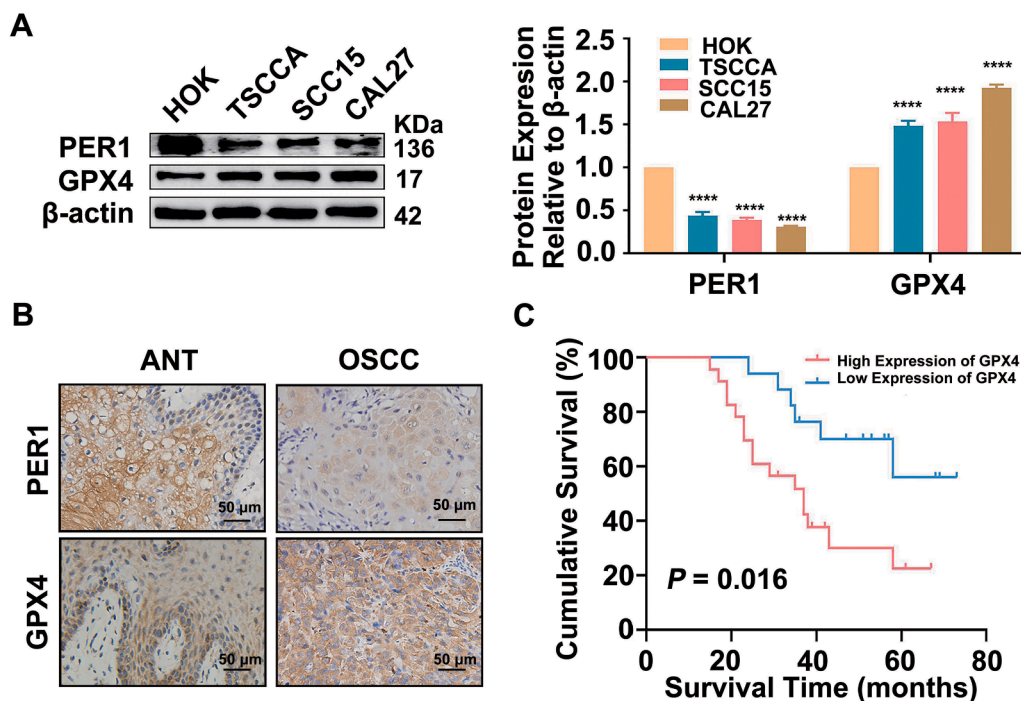


**Fig. 1.** Expression of PER1 and GPX4 in OSCC cells and tissues and analysis of clinical significance. (A) Western blotting showed that PER1 protein expression in OSCC cells was significantly reduced, while GPX4 expression was significantly increased. (B) Immunohistochemistry showed that PER1 protein expression in OSCC tissue ( $n = 40$ ) decreased significantly, while GPX4 expression increased significantly. (C) The survival time of OSCC patients with high GPX4 expression was significantly shorter than that of OSCC patients with low GPX4 expression. All data are representative of 3 independent experiments. Data are shown as the mean  $\pm$  SD ( $n \geq 3$ ). \* $P < 0.05$ ; \*\* $P < 0.01$ ; \*\*\* $P < 0.001$ ; \*\*\*\* $P < 0.0001$ . ANT, adjacent non-cancerous tissues.

magnetic beads and co-IP samples were detected by Western blotting.

*Dual luciferase reporter assay*

The PER1-luc plasmid and Renilla luciferase plasmid were cotransfected into TSCCA. The vector plasmid and Renilla luciferase plasmid were cotransfected as a negative control. The firefly luciferase activity

**Table 1**

The relationship between GPX4 expression and clinicopathological features of patients with OSCC.

Parameters	Total	GPX4 Expression		$\chi^2$	P value
		Low	High		
Age				0.63	0.73
≥60	5	2	3		
45–60	19	7	12		
<45	16	8	8		
Gender				0.017	0.896
Male	24	10	14		
Female	16	7	9		
Tumor Differentiation				2.063	0.356
Well	16	9	7		
Moderate	18	6	12		
Poor	6	2	4		
T Stage				21.909	<0.01
T1	5	5	0		
T2	19	12	7		
T3	13	0	13		
T4	3	0	3		
lymph node metastasis				6.812	0.009
Yes	21	13	8		
No	19	4	15		
Clinical Stage				19.742	<0.01
I	5	5	0		
II	10	8	2		
III	11	2	9		
IV	14	2	12		
Site				3.6	0.463
Gingival	7	2	5		
Tongue	15	6	9		
Buccal	10	6	4		
Palate	3	2	1		
Floor of the Oral	5	1	4		

(F), and Renilla luciferase activity (R) were detected. Relative luciferase activity = F/R.

*Chromatin immunoprecipitation assay (ChIP)*

The ChIP experiment was performed according to the manufacturer’s instructions for the ChIP Assay Kit (P2078, Beyotime). The primers for the PER1 promoter sequence were shown in Supplementary Table 4.

*Cycloheximide (CHX) chase experiments*

The cells were cultured with cycloheximide (Sigma-Aldrich, USA). Total protein was extracted at different time points and was detected by Western blotting.

*Tumor formation experiment in vivo*

Ten SPF BALB/c-nu male nude mice in experimental group (OE-PER1-SCC15) and control group (vector-SCC15) were injected subcutaneously with OE-PER1-SCC15 and vector-SCC15 cells respectively, and then killed by cervical dislocation on the 25th day. The weight, maximum long diameter (a) and minimum short diameter (b) of the tumor were measured. Tumor volume =  $0.5 \times a \times b^2$ . Animal experiments were approved by the Laboratory Animal Use Management Committee of the Laboratory Animal Research Institute of Chongqing Medical University (approval number: 2018–102) and were conducted as per the guidelines of the committee.

*Statistical analysis*

GraphPad Prism 9.0 (GraphPad Software, La Jolla, CA) was used for statistical analysis. The experimental data results of every 3 independent replicates are presented as the mean  $\pm$  SD. Student’s t-test was used for comparisons between two independent sample groups. One-way ANOVA test was used for one-way comparisons between multiple groups, and two-way ANOVA test was used for two-way comparisons between multiple groups. The Spearman rank correlation test was used for correlation analysis of protein expression. The chi-square test was



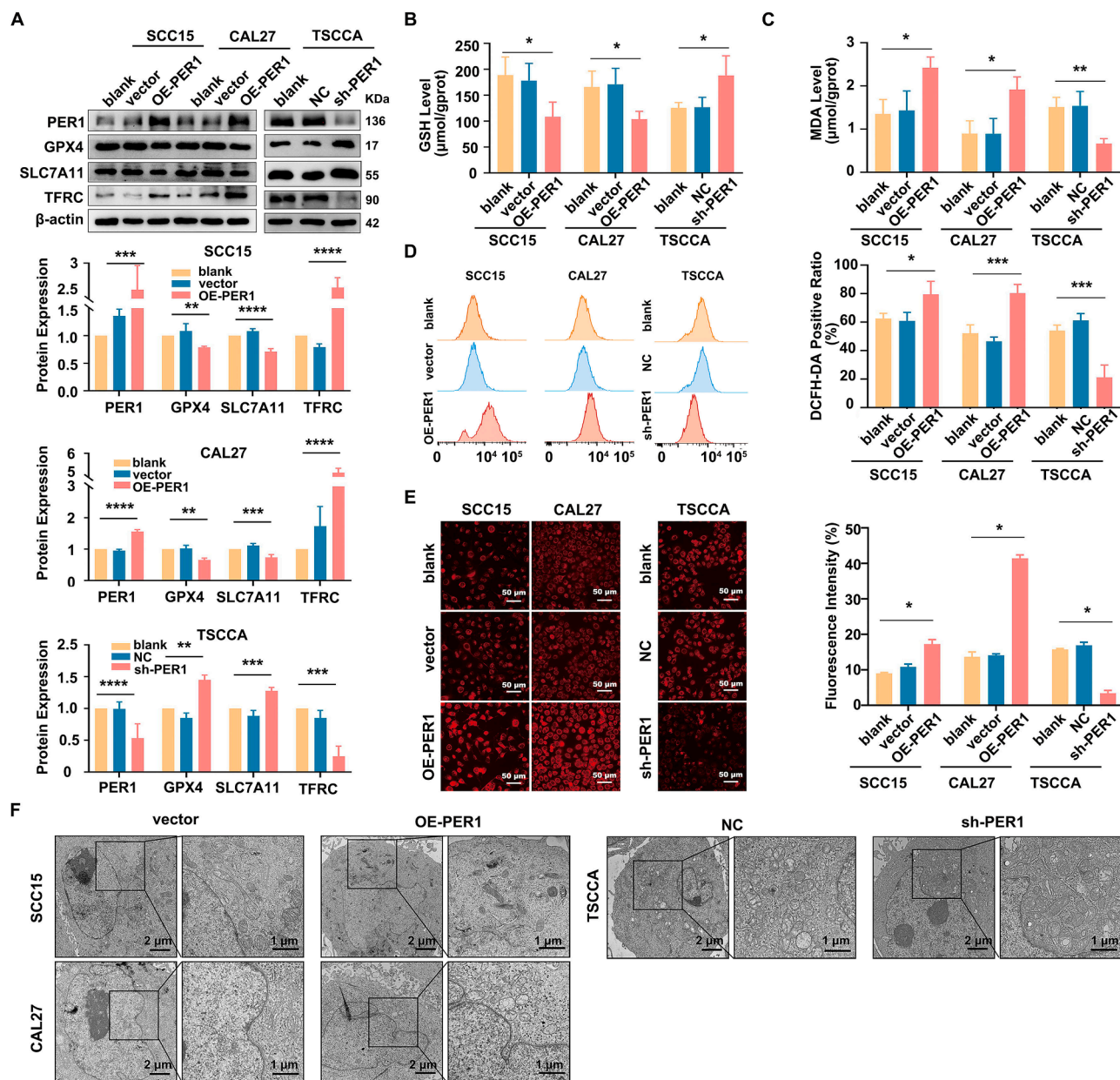


**Fig. 2.** PER1 promotes ferroptosis in OSCC cells. (A) Western blotting showed that TFRC protein expression significantly increased in the OE-PER1-SCC15 and OE-PER1-CAL27 cells and decreased significantly in the sh-PER1-TSCCA cells; SLC7A11 and GPX4 protein levels were decreased significantly in the OE-PER1-SCC15 and OE-PER1-CAL27 cells and significantly increased in the sh-PER1-TSCCA cells. (B) GSH content detection showed that GSH levels were significantly reduced in the OE-PER1-SCC15 and OE-PER1-CAL27 cells and significantly increased in the sh-PER1-TSCCA cells. (C) MDA content detection showed that MDA levels increased significantly in the OE-PER1-SCC15 and OE-PER1-CAL27 cells and decreased significantly in the sh-PER1-TSCCA cells. (D) Flow cytometry showed that ROS levels increased significantly in the OE-PER1-SCC15 and OE-PER1-CAL27 cells and decreased significantly in the sh-PER1-TSCCA cells. (E) The fluorescence intensity of Fe<sup>2+</sup> stained by FerroOrange was significantly enhanced in the OE-PER1-SCC15 and OE-PER1-CAL27 cells but was significantly reduced in the sh-PER1-TSCCA cells. (F) Shrunken mitochondria, increased membrane density, and decreased cristae were shown in the OE-PER1-SCC15 and OE-PER1-CAL27 cells under TEM. There was no significant change in mitochondrial morphology in the sh-PER1-TSCCA cells. All data are representative of 3 independent experiments. Data are shown as the mean ± SD (n ≥ 3). \*P < 0.05; \*\*P < 0.01; \*\*\*P < 0.001; \*\*\*\*P < 0.0001.

used to examine the relationship between GPX4 expression level and clinicopathological parameters. The Kaplan-Meier method was used to draw the survival curve, and the log-rank test method was used to analyze the statistical significance of the difference in survival time between the two groups. P < 0.05 was considered statistically significant.

## Results

### Expression of PER1 and GPX4 in OSCC cells and tissues and analysis of clinical significance

To evaluate the correlations between PER1 and ferroptosis, we first detected the expression of PER1 and a key ferroptosis protein, glutathione peroxidase (GPX4), in OSCC cells. Western blotting results showed that compared with that in normal HOK oral mucosal cells, PER1 expression in the OSCC cell lines TSCCA, SCC15 and CAL27 was



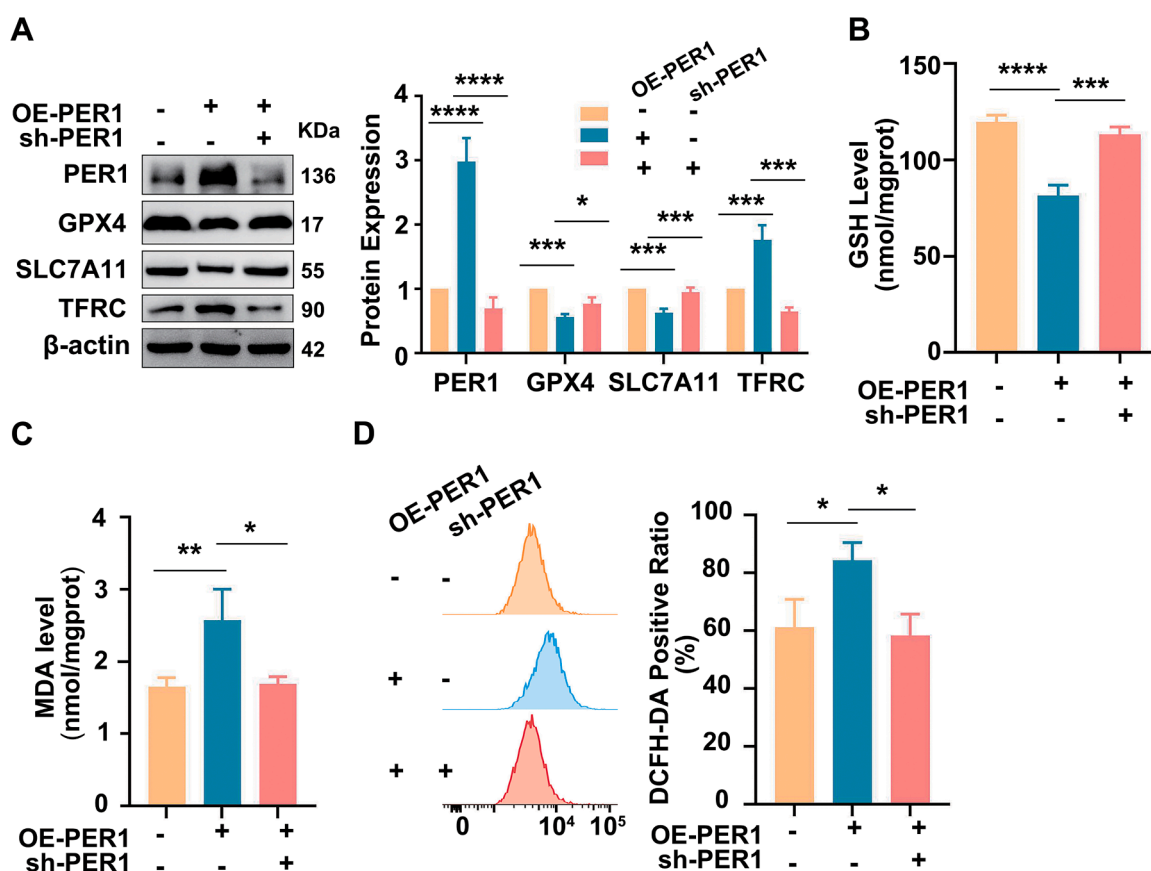


**Fig. 3.** Ferropromoted in OE-PER1 SCC15 cells is reversed when PER1 is knocked down. (A) Western blotting showed that after PER1 silencing in the OE-PER1-SCC15 cells, PER1 overexpression increased TFRC protein expression and decreased SLC7A11 and GPX4 protein levels were rescued. (B-D) After silencing of PER1 in the OE-PER1-SCC15 cells, PER1 overexpression decreased the GSH levels (B) and increased MDA levels (C), and ROS levels (D) were reversed. All data are representative of 3 independent experiments. Data are shown as the mean  $\pm$  SD ( $n \geq 3$ ). \* $P < 0.05$ ; \*\* $P < 0.01$ ; \*\*\* $P < 0.001$ ; \*\*\*\* $P < 0.0001$ .

significantly reduced, while GPX4 expression was significantly increased ( $P < 0.01$ ) (Fig. 1A).

We further evaluated the expression of PER1 and GPX4 in cancer tissues of OSCC patients. The immunohistochemistry results of cancer tissues from 40 OSCC patients showed that PER1 expression was significantly reduced ( $P < 0.05$ ), while GPX4 expression was significantly increased ( $P < 0.05$ ) (Fig. 1B). The expression levels of PER1 and GPX4 were significantly negatively correlated ( $P < 0.01$ ) (Supplementary Table 5). Moreover, GPX4 expression was significantly correlated with OSCC tumor size, cervical lymph node metastasis, and TNM staging ( $P < 0.05$ ) (Table 1); Kaplan–Meier survival analysis of these forty OSCC showed that the average overall survival time (OS) of OSCC patients with high GPX4 expression was significantly shorter than those with low expression ( $P < 0.05$ ) (Fig. 1C).

These results suggest that ferroptosis plays an important role in the initiation and development of OSCC and may be negatively regulated by PER1.

#### PER1 promotes ferroptosis in OSCC cells

To explore the regulation of ferroptosis by PER1 in OSCC cells, we detected the expression of the key ferroptosis-related proteins GPX4, solute carrier family 7 member 11 (SLC7A11) and transferrin receptor (TFRC), detected the levels of GSH, MDA, ROS and  $Fe^{2+}$ , and observed mitochondrial morphology in OSCC cells with overexpression or silencing of PER1. The results showed that compared with those of the control group, the levels of GPX4, SLC7A11 and GSH were significantly

reduced ( $P < 0.05$ ), and the levels of TFRC, MDA, ROS and  $Fe^{2+}$  were significantly increased ( $P < 0.05$ ) in the OE-PER1-SCC15 and OE-PER1-CAL27 cells (Fig. 2A-E). Shrunken mitochondria, increased membrane density, and decreased cristae were observed in the OE-PER1 cells by transmission electron microscopy (Fig. 2F). In the sh-PER1-TSCCA cells, the levels of GPX4, SLC7A11, and GSH were significantly increased ( $P < 0.05$ ), and the levels of TFRC, MDA, ROS, and  $Fe^{2+}$  were significantly reduced ( $P < 0.05$ ) (Fig. 2A-E), while no obvious change was found in mitochondrial morphology (Fig. 2F).

Further verification was performed in the OE-PER1-SCC15 cells infected with sh-PER1 lentivirus to silence PER1 again. The results showed that compared with those in SCC15 cells, the levels of GPX4, SLC7A11 and GSH in the OE-PER1-SCC15 cells were significantly reduced ( $P < 0.05$ ), and the levels of TFRC, MDA and ROS were significantly increased ( $P < 0.05$ ). However, silencing PER1 in the OE-PER1-SCC15 cells significantly rescued these effects ( $P < 0.05$ ) (Fig. 3).

These results indicate that PER1 overexpression promotes ferroptosis, while PER1 silencing inhibits ferroptosis in OSCC cells.

#### PER1 promotes OSCC cell ferroptosis via HIF-1 $\alpha$ in vitro and in vivo

Current studies have shown that HIF-1 $\alpha$  is an important pathway regulating ferroptosis [25]. However, whether PER1 can regulate HIF-1 $\alpha$  is still unknown in OSCC. Therefore, we detected HIF-1 $\alpha$  mRNA and protein expression in OSCC cells with overexpression or silencing of PER1. The results showed that HIF-1 $\alpha$  protein in the OE-PER1-SCC15 and OE-PER1-CAL27 cells was significantly reduced ( $P < 0.01$ ), and

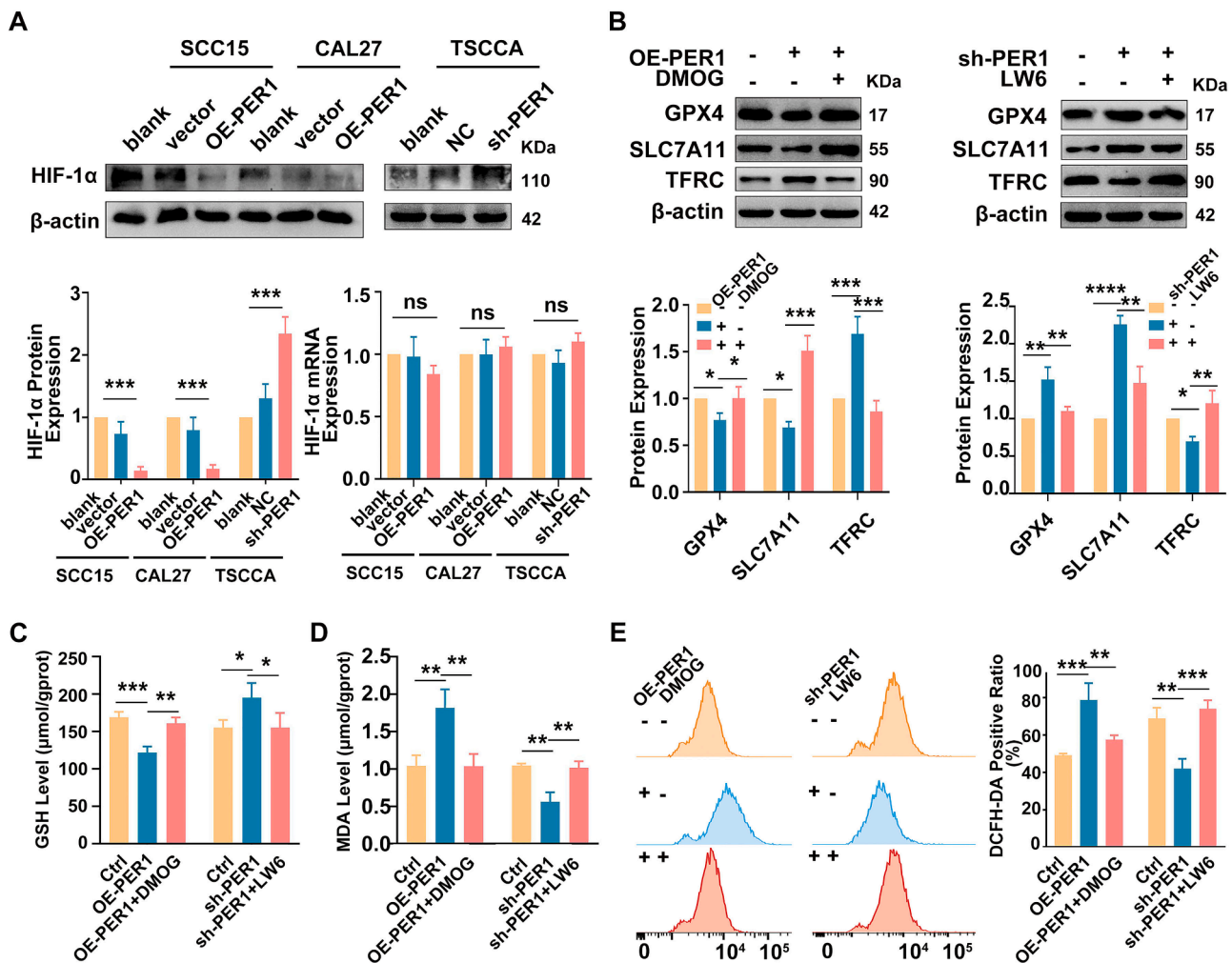


**Fig. 4.** PER1 promotes OSCC cell ferroptosis via HIF-1 $\alpha$ . (A) Western blotting showed that HIF-1 $\alpha$  protein expression was significantly reduced in the OE-PER1-SCC15 and OE-PER1-CAL27 cells and significantly increased in the sh-PER1-TSCCA cells, while HIF-1 $\alpha$  mRNA expression was not significantly changed. (B) Western blotting showed that after the OE-PER1-SCC15 cells were treated with DMOG, the increase in TFRC expression and the decrease in SLC7A11 and GPX4 expression caused by PER1 overexpression were reversed; after the sh-PER1-TSCCA cells were treated with LW6, the decrease in TFRC expression and the increase in SLC7A11 and GPX4 expression caused by PER1 silencing were reversed. (C-E) After the OE-PER1-SCC15 cells were treated with DMOG, the decreased GSH level (C) and increased MDA (D) and ROS levels (E) caused by PER1 overexpression were reversed. After the sh-PER1-TSCCA cells were treated with LW6 and the increased GSH level (B) and decreased MDA (C) and ROS levels (D) caused by PER1 silencing were reversed. All data are representative of 3 independent experiments. Data are shown as the mean  $\pm$  SD ( $n \geq 3$ ). \* $P < 0.05$ ; \*\* $P < 0.01$ ; \*\*\* $P < 0.001$ ; \*\*\*\* $P < 0.0001$ . ANT, adjacent non-cancerous tissues.

HIF-1 $\alpha$  protein expression in the sh-PER1-TSCCA cells was significantly increased ( $P < 0.01$ ) (Fig. 4A), while the HIF-1 $\alpha$  mRNA levels did not change significantly in OSCC cells with either overexpression or silencing of PER1 ( $P > 0.05$ ) (Fig. 4A). These results indicate that PER1 can regulate HIF-1 $\alpha$  protein levels, but not HIF-1 $\alpha$  mRNA levels.

To explore whether PER1 regulates the ferroptosis of OSCC cells through HIF-1 $\alpha$ , we cultured PER1-overexpressing or PER1-silenced OSCC cells with the HIF-1 $\alpha$  activator DMOG (China, Selleck, S7483) or the HIF-1 $\alpha$  inhibitor LW6 (China, Selleck, S8441) to detect changes in ferroptosis. The results showed that after DMOG (1 mM, 24 h) treatment, the decreased levels of GPX4, SLC7A11 and GSH, as well as the increased levels of TFRC, MDA and ROS were significantly restored in the OE-PER1-SCC15 cells ( $P < 0.05$ ) (Fig. 4B-E). After LW6 (20  $\mu$ M, 24 h) treatment of the sh-PER1-TSCCA cells, the increased levels of GPX4, SLC7A11, and GSH, as well as the decreased levels of TFRC, MDA, and ROS recovered significantly ( $P < 0.05$ ) (Fig. 4B-E).

These effects were further verified through subcutaneous tumor formation assays *in vivo*. The results showed that the growth rate, tumor weight and volume of subcutaneous tumors in the OE-PER1-SCC15 group were significantly lower than those in the vector group ( $P <$

0.01) (Fig. 5A-C). In the tumors of the OE-PER1-SCC15 group, TFRC protein expression was significantly increased, and GPX4 and HIF-1 $\alpha$  protein levels were significantly decreased ( $P < 0.05$ ) (Fig. 5D). In addition, the IHC results in the cancer tissues of the 40 OSCC patients showed that PER1 expression was significantly reduced (Fig. 1B) and HIF-1 $\alpha$  expression was significantly increased ( $P < 0.05$ ) (Fig. 5E). The expression levels of PER1 and HIF-1 $\alpha$  were significantly negatively correlated ( $P < 0.05$ ) (Supplementary Table 5), while HIF-1 $\alpha$  and GPX4 expression levels were significantly positively correlated ( $P < 0.05$ ) (Supplementary Table 6).

These results indicate that PER1 regulates the ferroptosis of OSCC cells via HIF-1 $\alpha$  *in vitro* and *in vivo*.

#### PER1 binds with HIF-1 $\alpha$ and promotes HIF-1 $\alpha$ degradation

We previously showed that in OSCC cells, overexpression or silencing of PER1 leads to a significant decrease or increase in HIF-1 $\alpha$  protein, respectively, but there was no significant change in the level of HIF-1 $\alpha$  mRNA (Fig. 4A). Therefore, we explored the mechanism of PER1 in HIF-1 $\alpha$  regulation based on protein interactions. Co-IP results showed

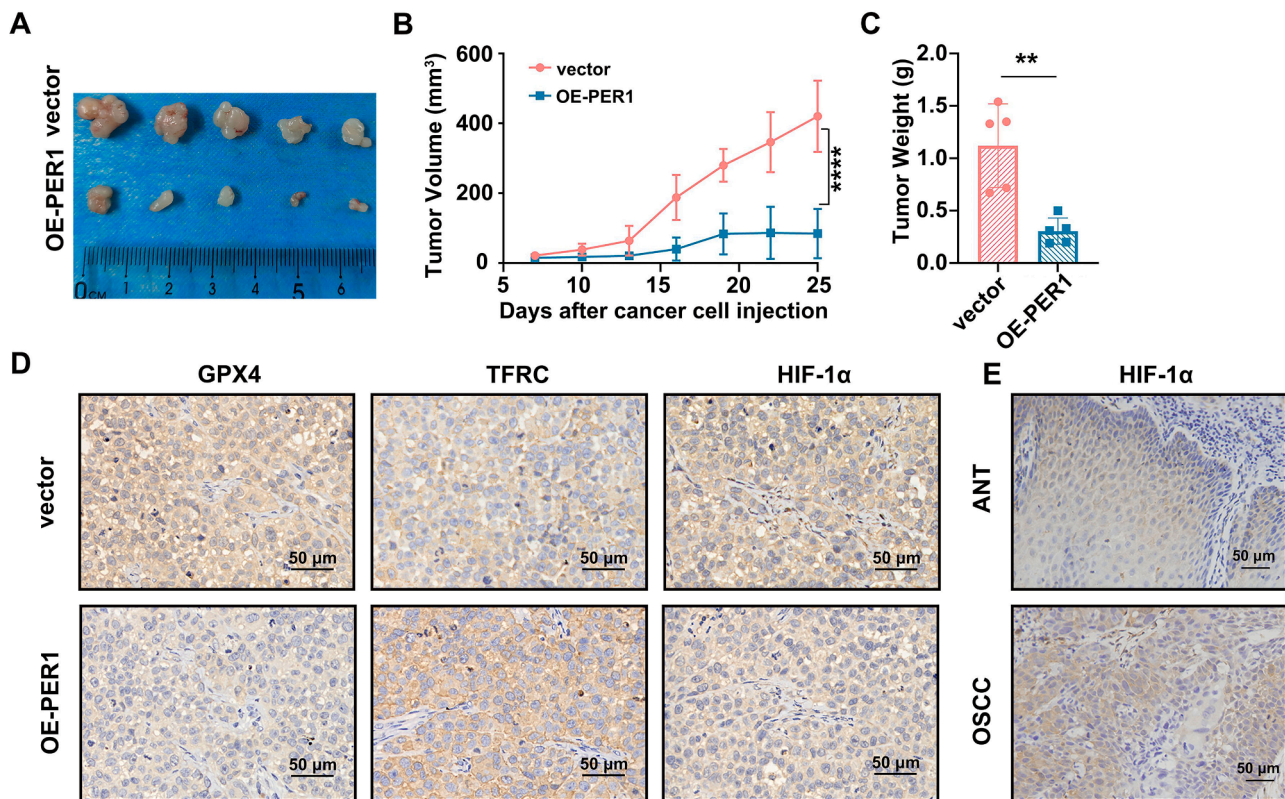


**Fig. 5.** PER1 inhibits OSCC *in vivo*. (A–C) Subcutaneous tumor formation assays in nude mice showed that the volume and weight of tumors in the OE-PER1-SCC15 group increased significantly. (D) The expression of GPX4 and HIF-1 $\alpha$  in the OE-PER1-SCC15 group was decreased, and TFRC expression was increased in the tumors. (E) HIF-1 $\alpha$  expression in tumor tissues of OSCC patients ( $n = 40$ ) was significantly higher than that in adjacent tissues. All data are representative of 3 independent experiments. Data are shown as the mean  $\pm$  SD ( $n \geq 3$ ). \* $P < 0.05$ ; \*\* $P < 0.01$ ; \*\*\* $P < 0.001$ ; \*\*\*\* $P < 0.0001$ . ANT, adjacent non-cancerous tissues.

that in SCC15 cells, PER1 could bind to HIF-1 $\alpha$  (Fig. 6A). The CHX tracking assays proved that, the half-life of the HIF-1 $\alpha$  protein in the OE-PER1-SCC15 cells was significantly shorter than that of the SCC15 cells ( $P < 0.05$ ) (Fig. 6B). The shorter half-life of the HIF-1 $\alpha$  protein was significantly restored after PER1 knockdown in the OE-PER1-SCC15 cells ( $P < 0.05$ ) (Fig. 6B). These results indicate that the binding of PER1 with HIF-1 $\alpha$  promotes the degradation of HIF-1 $\alpha$ .

#### HIF-1 $\alpha$ inhibits PER1 transcription

Considering that HIF-1 $\alpha$  is a transcription factor that regulates many important biological functions [28,32], we used the databases JASPAR (<http://jaspar.genereg.net/>) and animal TFDB (<http://bioinfo.life.hust.edu.cn/AnimalTFDB/#/>) to explore its target genes. Interestingly, there were multiple HIF-1 $\alpha$  binding sites on the PER1 promoter (Fig. 6C). This finding suggests that HIF-1 $\alpha$  may have feedback transcriptional regulation on PER1. To confirm this transcriptional regulation, we detected PER1 expression in TSCCA cells cultured with the HIF-1 $\alpha$  activator DMOG. The results showed that after treatment with DMOG, the PER1 mRNA and protein levels in TSCCA cells were significantly reduced ( $P < 0.01$ ) (Fig. 6D–E). Then, we established TSCCA cells overexpressing HIF-1 $\alpha$  (OE-HIF-1 $\alpha$ -TSCCA). RT-qPCR results showed that PER1 mRNA was significantly reduced in the OE-HIF-1 $\alpha$ -TSCCA cells ( $P < 0.01$ ) (Fig. 6F). Western blotting showed that PER1 and TFRC protein levels were significantly reduced, and GPX4 and SLC7A11 protein levels were significantly increased in the OE-HIF-1 $\alpha$ -TSCCA cells ( $P < 0.01$ ) (Fig. 6G–H). Furthermore, the transcriptional regulatory effect of HIF-1 $\alpha$  on PER1 was confirmed with ChIP and dual luciferase reporter assays. ChIP results showed that HIF-1 $\alpha$  can bind to the PER1 promoter in TSCCA cells (Fig. 6I). The dual luciferase reporter assay showed that the relative fluorescence intensity of the PER1 promoter in the

OE-HIF-1 $\alpha$ -TSCCA cells was significantly reduced compared with that in the TSCCA cells ( $P < 0.01$ ) (Fig. 6J).

These results prove that in OSCC cells, HIF-1 $\alpha$  can bind to the PER1 promoter to inhibit PER1 transcription, and that PER1 and HIF-1 $\alpha$  form a PER1/HIF-1 $\alpha$  negative feedback loop to regulate ferroptosis.

#### Discussion

At present, it has been proven that the core circadian clock gene PER1 is involved in the regulation of apoptosis, autophagy and DNA damage repair as well as other important physiological processes [16, 33–34], and its abnormal expression plays an important role in the occurrence and development of many cancers such as gastric cancer and non-small cell lung cancer [13–16]. We found that PER1 is expressed at low levels in OSCC tissues and is significantly related to the clinical stage and survival time of OSCC patients [17, 18]. These studies suggest that PER1 has an important and extensive tumor suppressor effect, and in-depth PER1 research may have important prospects for clinical translation. This study showed for the first time that PER1 can regulate cell ferroptosis. We have proven that low PER1 expression in OSCC inhibits ferroptosis and promotes tumor growth *in vivo* and *in vitro*. The binding of HIF-1 $\alpha$  and PER1 forms a PER1/HIF-1 $\alpha$  negative feedback loop, which amplifies the effect of PER1 on inhibiting ferroptosis in cancer cells. Our findings contribute to a complementary understanding of the mechanism of cancer.

Ferroptosis is a newly discovered mode of cell death that differs from other forms of cell death such as apoptosis, autophagy and necrosis in cell morphology, biochemistry, and genes [19, 20]. Deeper research may provide new targets and strategies for the treatment of cancer. The main feature of ferroptosis is that excess accumulation of iron-dependent lipid peroxides leads to cell death. Ferroptosis is a complicated process and



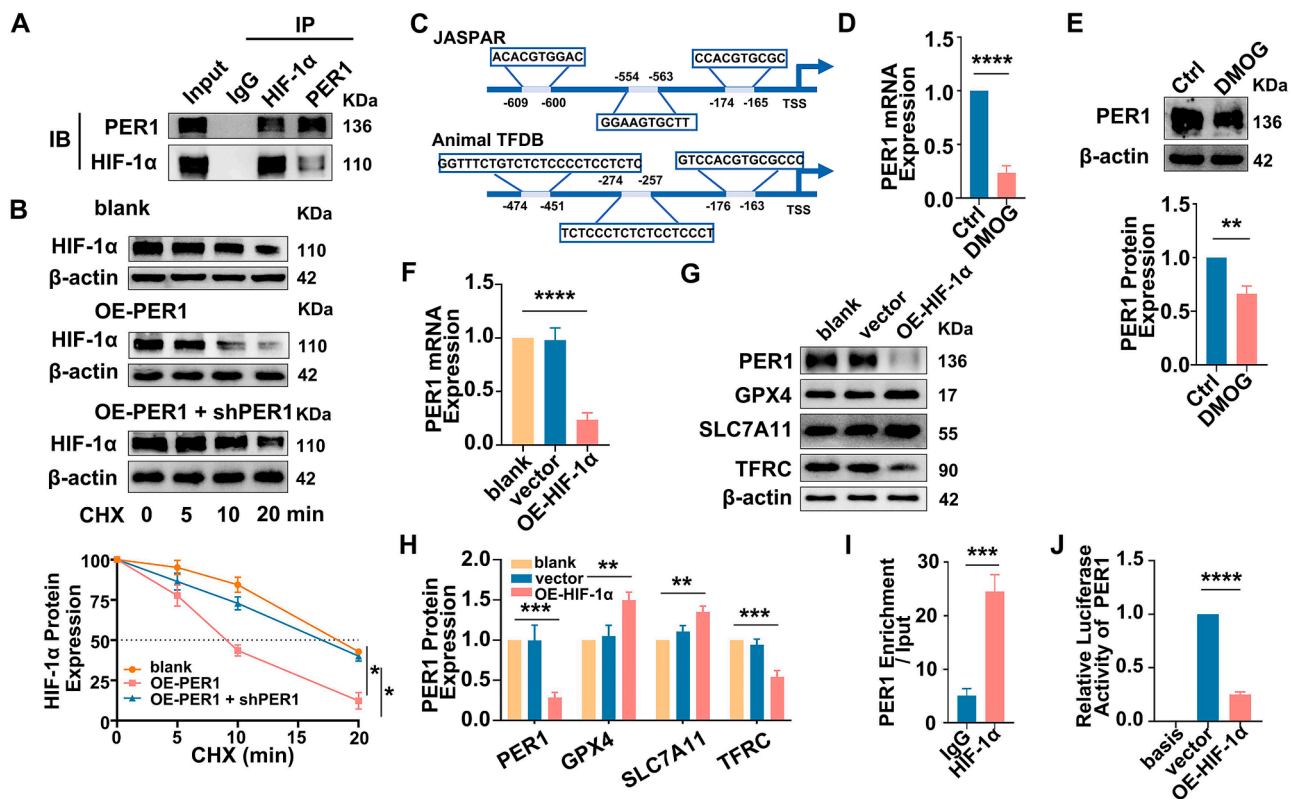


**Fig. 6.** PER1 forms a negative feedback loop with HIF-1 $\alpha$ . (a) Co-IP shows that in SCC15 cells, PER1 binds with HIF-1 $\alpha$  to form a PER1/HIF-1 $\alpha$  complex. (b) CHX tracking experiments proved that the half-life of HIF-1 $\alpha$  protein in the OE-PER1-SCC15 cells was significantly shortened and recovered significantly after PER1 was silenced in the OE-PER1-SCC15 cells. (c) Schematic diagrams of the binding sites of HIF-1 $\alpha$  protein and the PER1 promoter. (d-e) PER1 mRNA and protein levels in TSCCA cells treated with DMOG were significantly reduced. (f-h) PER1 mRNA expression was significantly reduced in the OE-HIF-1 $\alpha$ -TSCCA cells (f), and PER1 and TFRC protein levels were significantly reduced, while GPX4 and SLC7A11 protein levels were significantly increased (gh). (i) ChIP showed that HIF-1 $\alpha$  protein binds to the PER1 promoter. (j) The dual luciferase reporter assay showed that the relative fluorescence intensity of PER1 in the OE-HIF-1 $\alpha$ -TSCCA cells was significantly reduced. All data are representative of 3 independent experiments. Data are shown as the mean  $\pm$  SD ( $n \geq 3$ ). \* $P < 0.05$ ; \*\* $P < 0.01$ ; \*\*\* $P < 0.001$ ; \*\*\*\* $P < 0.0001$ . CHX, Cycloheximide.

involves glutathione depletion, decreased glutathione peroxidase (GPX4) activity, and inhibition of the cell antioxidant capacity, which lead to enhanced lipid peroxidation (LPO) and increased lipid reactive oxygen species (ROS), eventually triggering cell death [19]. Current studies have shown that ferroptosis plays important roles in the occurrence and development of lung cancer, gastric cancer, OSCC and other tumors [21–24]. In this study, we proved the role of PER1 in regulating the ferroptosis of OSCC cells based on cell morphology, biochemistry and gene changes. We found that the levels of GPX4, SLC7A11, and GSH decreased, and the levels of TFRC, ROS, and Fe<sup>2+</sup> increased in the OSCC cells overexpressing PER1. Shrunken mitochondria, increased membrane density, and decreased cristae were shown in the OE-PER1 OSCC cells, which proved that PER1 promotes ferroptosis. We also obtained the opposite results in the PER1-silenced OSCC cells. Moreover, *in vivo* assays have verified these effects.

Exploring the molecular mechanisms that regulate ferroptosis may be a way to find new targets for the treatment of cancer. HIF-1 $\alpha$  is an important pathway involved in the regulation of ferroptosis [25–27]. To explore whether PER1 can regulate ferroptosis through HIF-1 $\alpha$ , we proved that HIF-1 $\alpha$  mRNA expression did not change in OSCC cells overexpressing or silencing PER1, but HIF-1 $\alpha$  protein expression decreased or increased, respectively. Furthermore, after addition of HIF-1 $\alpha$  agonists or inhibitors to OSCC cells with overexpression or silencing of PER1, the changes in ferroptosis were significantly reversed. These results prove that PER1 regulates the ferroptosis of OSCC cells via HIF-1 $\alpha$ . Chilov, D., et al. reported that PER1 protein can bind to HIF-1 $\alpha$  protein in mouse brain tissue [30], but the functional effect of the binding of PER1 and HIF-1 $\alpha$  is still unclear. We further confirmed

through co-IP and CHX tracking experiments that PER1 combined with HIF-1 $\alpha$  promotes HIF-1 $\alpha$  degradation (the HIF-1 $\alpha$  half-life is shortened) and promotes ferroptosis in OSCC cells. HIF-1 $\alpha$  is an important transcription factor [28, 32]. Yu, C., et al. reported that PER1 mRNA expression decreased after HIF-1 $\alpha$  was overexpressed in liver cancer cells [35]. Our research also found that PER1 mRNA and protein expression decreased and cell ferroptosis was inhibited after overexpression of HIF-1 $\alpha$  in OSCC cells. We further proved that HIF-1 $\alpha$  can bind to the PER1 promoter to inhibit PER1 transcription using ChIP and dual luciferase reporter assays. Based on the results above, we firstly proved that in OSCC, the binding of PER1 and HIF-1 $\alpha$  forms a PER1/HIF-1 $\alpha$  negative feedback loop to amplify the effect of PER1 on regulating ferroptosis in cancer cells. However, there are still some limitations in this study. Current researches show that the main mechanisms of protein degradation are the autophagic pathway and ubiquitin-dependent proteasome pathway [36]. In this study, the pathway through which PER1 and HIF-1 $\alpha$  are combined to promote HIF-1 $\alpha$  degradation needs to be further studied.

In summary, this study demonstrated for the first time that the core circadian clock gene PER1 regulates ferroptosis in OSCC cells in a HIF-1 $\alpha$ -dependent manner *in vitro* and *in vivo* and that the binding of the PER1 and HIF-1 $\alpha$  proteins promotes HIF-1 $\alpha$  degradation. Moreover, HIF-1 $\alpha$  binds to the PER1 promoter to inhibit PER1 transcription. PER1 binds with HIF-1 $\alpha$  to form a PER1/HIF-1 $\alpha$  negative feedback loop to amplify the effect of PER1 on regulating ferroptosis in cancer cells. These findings suggest that targeted regulation of the PER1/HIF-1 $\alpha$  loop may provide a valuable new strategy for OSCC treatment in the future.

## Author contributions

K.Y. conceived the study, analyzed the data, and revised the paper; Y. Y. performed experiments, analyzed the data, and wrote the paper; H.T. and J.Z. assisted in experiments and analyzed the data.

## Declaration of Competing Interests

The authors declare that they have no known competing financial interests or personal relationships that could have appeared to influence the work reported in this paper.

## Acknowledgments

This work was supported by Chongqing Talents · Innovation Leading Talents Project (CQYC20200303128); Natural Science Foundation of Chongqing, China (cstc2018jcyjAX0208).

## Supplementary materials

Supplementary material associated with this article can be found, in the online version, at doi:10.1016/j.tranon.2022.101360.

## References

- [1] F. Bray, J. Ferlay, I. Soerjomataram, R.L. Siegel, L.A. Torre, A. Jemal, Global cancer statistics 2018: GLOBOCAN estimates of incidence and mortality worldwide for 36 cancers in 185 countries, *CA Cancer J. Clin.* 68 (2018) 394–424.
- [2] H. Sung, J. Ferlay, R.L. Siegel, M. Laversanne, I. Soerjomataram, A. Jemal, F. Bray, Global cancer statistics 2020: GLOBOCAN estimates of incidence and mortality worldwide for 36 cancers in 185 countries, *CA Cancer J. Clin.* 71 (2021) 209–249.
- [3] A.C. Chi, T.A. Day, B.W. Neville, Oral cavity and oropharyngeal squamous cell carcinoma—an update, *CA Cancer J. Clin.* 65 (2015) 401–421.
- [4] R.L. Siegel, K.D. Miller, H.E. Fuchs, A. Jemal, Cancer Statistics, *CA Cancer J. Clin.* 71 (2021) 7–33, 2021.
- [5] M. Mascitti, G. Orsini, V. Tosco, R. Monterubbani, A. Balercia, A. Putignano, M. Procaccini, A. Santarelli, An overview on current non-invasive diagnostic devices in oral oncology, *Front. Physiol.* 9 (2018) 1510.
- [6] M. Cristaldi, R. Mauceri, O. Di Fede, G. Giuliana, G. Campisi, V. Panzarella, Salivary biomarkers for oral squamous cell carcinoma diagnosis and follow-up: current status and perspectives, *Front. Physiol.* 10 (2019) 1476.
- [7] J.A. Mohawk, C.B. Green, J.S. Takahashi, Central and peripheral circadian clocks in mammals, *Annu. Rev. Neurosci.* 35 (2012) 445–462.
- [8] C. Dibner, U. Schibler, U. Albrecht, The mammalian circadian timing system: organization and coordination of central and peripheral clocks, *Annu. Rev. Physiol.* 72 (2010) 517–549.
- [9] S. Chakrabarti, F. Michor, Circadian clock effects on cellular proliferation: insights from theory and experiments, *Curr. Opin. Cell Biol.* 67 (2020) 17–26.
- [10] H. Reinke, G. Asher, Crosstalk between metabolism and circadian clocks, *Nat. Rev. Mol. Cell Biol.* 20 (2019) 227–241.
- [11] G. Sulli, M.T.Y. Lam, S. Panda, Interplay between circadian clock and cancer: new frontiers for cancer treatment, *Trends Cancer* 5 (2019) 475–494.
- [12] E. Cash, S. Sephton, C. Woolley, A.M. Elbehi, R. I.A. B. Ekine-Afolabi, V.C. Kok, The role of the circadian clock in cancer hallmark acquisition and immune-based cancer therapeutics, *J. Exp. Clin. Cancer Res.* 40 (2021) 119.
- [13] S. Gery, N. Komatsu, N. Kawamata, C.W. Miller, J. Desmond, R.K. Virk, A. Marchevsky, R. McKenna, H. Taguchi, H.P. Koeffler, Epigenetic silencing of the candidate tumor suppressor gene Per1 in non-small cell lung cancer, *Clin. Cancer Res.* 13 (2007) 1399–1404.
- [14] B. Liu, K. Xu, Y. Jiang, X. Li, Aberrant expression of Per1, Per2 and Per3 and their prognostic relevance in non-small cell lung cancer, *Int. J. Clin. Exp. Pathol.* 7 (2014) 7863–7871.
- [15] H. Zhao, Z.L. Zeng, J. Yang, Y. Jin, M.Z. Qiu, X.Y. Hu, J. Han, K.Y. Liu, J.W. Liao, R. H. Xu, Q.F. Zou, Prognostic relevance of Period1 (Per1) and Period2 (Per2) expression in human gastric cancer, *Int. J. Clin. Exp. Pathol.* 7 (2014) 619–630.
- [16] S. Gery, N. Komatsu, L. Baldjyan, A. Yu, D. Koo, H.P. Koeffler, The circadian gene Per1 plays an important role in cell growth and DNA damage control in human cancer cells, *Mol. Cell.* 22 (2006) 375–382.
- [17] G. Yang, Y. Yang, H. Tang, K. Yang, Loss of the clock gene Per1 promotes oral squamous cell carcinoma progression via the AKT/mTOR pathway, *Cancer Sci.* 111 (2020) 1542–1554.
- [18] R. Chen, K. Yang, N.B. Zhao, D. Zhao, D. Chen, C.R. Zhao, H. Tang, Abnormal expression of PER1 circadian-clock gene in oral squamous cell carcinoma, *Onco. Targets Ther.* 5 (2012) 403–407.
- [19] S.J. Dixon, K.M. Lemberg, M.R. Lamprecht, R. Skouta, E.M. Zaitsev, C.E. Gleason, D.N. Patel, A.J. Bauer, A.M. Cantley, W.S. Yang, B. Morrison 3rd, B.R. Stockwell, Ferroptosis: an iron-dependent form of nonapoptotic cell death, *Cell* 149 (2012) 1060–1072.
- [20] B.R. Stockwell, J.P. Friedmann Angeli, H. Bayir, A.I. Bush, M. Conrad, S.J. Dixon, S. Fulda, S. Gascón, S.K. Hatzios, V.E. Kagan, K. Noel, X. Jiang, A. Linkermann, M. E. Murphy, M. Overholtzer, A. Oyagi, G.C. Pagnussat, J. Park, Q. Ran, C. S. Rosenfeld, K. Salnikow, D. Tang, F.M. Torti, S.V. Torti, S. Toyokuni, K. A. Woerpel, D.D. Zhang, Ferroptosis: a regulated cell death nexus linking metabolism, *Redox Biol. Dis.*, *Cell* 171 (2017) 273–285.
- [21] M. Wang, C. Mao, L. Ouyang, Y. Liu, W. Lai, N. Liu, Y. Shi, L. Chen, D. Xiao, F. Yu, X. Wang, H. Zhou, Y. Cao, S. Liu, Q. Yan, Y. Tao, B. Zhang, Long noncoding RNA LINC00336 inhibits ferroptosis in lung cancer by functioning as a competing endogenous RNA, *Cell Death Differ.* 26 (2019) 2329–2343.
- [22] H. Zhang, T. Deng, R. Liu, T. Ning, H. Yang, D. Liu, Q. Zhang, D. Lin, S. Ge, M. Bai, X. Wang, L. Zhang, H. Li, Y. Yang, Z. Ji, H. Wang, G. Ying, Y. Ba, CAF secreted miR-522 suppresses ferroptosis and promotes acquired chemo-resistance in gastric cancer, *Mol. Cancer* 19 (2020) 43.
- [23] M. Fukuda, Y. Ogasawara, H. Hayashi, A. Okuyama, J. Shiono, K. Inoue, H. Sakashita, Down-regulation of glutathione peroxidase 4 in oral cancer inhibits tumor growth through SREBP1 signaling, *Anticancer Res.* 41 (2021) 1785–1792.
- [24] X. Wang, K. Liu, H. Gong, D. Li, W. Chu, D. Zhao, X. Wang, D. Xu, Death by histone deacetylase inhibitor quisinostat in tongue squamous cell carcinoma via apoptosis, pyroptosis, and ferroptosis, *Toxicol. Appl. Pharmacol.* 410 (2021), 115363.
- [25] X. Chen, R. Kang, G. Kroemer, D. Tang, Broadening horizons: the role of ferroptosis in cancer, *Nat. Rev. Clin. Oncol.* (2021).
- [26] M. Yang, P. Chen, J. Liu, S. Zhu, G. Kroemer, D.J. Klionsky, M.T. Lotze, H.J. Zeh, R. Kang, D. Tang, Clocked autophagy is a novel selective autophagy process favoring ferroptosis, *Sci. Adv.* 5 (2019) eaav2238.
- [27] Y. Zou, M.J. Palte, A.A. Deik, H. Li, J.K. Eaton, W. Wang, Y.Y. Tseng, R. Deasy, M. Kost-Alimova, V. Dancik, E.S. Leshchiner, V.S. Viswanathan, S. Signoretti, T. K. Choueiri, J.S. Boehm, B.K. Wagner, J.G. Doench, C.B. Clish, P.A. Clemons, S. L. Schreiber, A GPX4-dependent cancer cell state underlies the clear-cell morphology and confers sensitivity to ferroptosis, *Nat. Commun.* 10 (2019) 1617.
- [28] D.C. Bersten, A.E. Sullivan, D.J. Peet, M.L. Whitelaw, bHLH-PAS proteins in cancer, *Nat. Rev. Cancer* 13 (2013) 827–841.
- [29] B.L. Taylor, I.B. Zhulin, PAS domains: internal sensors of oxygen, redox potential, and light, *Microbiol. Mol. Biol. Rev.* 63 (1999) 479–506.
- [30] D. Chilov, T. Hofer, C. Bauer, R.H. Wenger, M. Gassmann, Hypoxia affects expression of circadian genes PER1 and CLOCK in mouse brain, *FASEB J.* 15 (2001) 2613–2622.
- [31] M. He, C. Zuo, J. Wang, J. Liu, B. Jiao, J. Zheng, Z. Cai, Prognostic significance of the aggregative perivascular growth pattern of tumor cells in primary central nervous system diffuse large B-cell lymphoma, *Neuro. Oncol.* 15 (2013) 727–734.
- [32] N. Albadari, S. Deng, W. Li, The transcriptional factors HIF-1 and HIF-2 and their novel inhibitors in cancer therapy, *Expert Opin. Drug Discov.* 14 (2019) 667–682.
- [33] Y. Han, F. Meng, J. Venter, N. Wu, Y. Wan, H. Standeford, H. Francis, C. Meiningner, J. Greene Jr., J.P. Trzeciakowski, L. Ehrlich, S. Glaser, G. Alpini, miR-34a-dependent overexpression of Per1 decreases cholangiocarcinoma growth, *J. Hepatol.* 64 (2016) 1295–1304.
- [34] N. Wiebking, E. Maronde, A. Rami, Increased neuronal injury in clock gene Per1 deficient-mice after cerebral ischemia, *Curr. Neurovasc. Res.* 10 (2013) 112–125.
- [35] C. Yu, S.L. Yang, X. Fang, J.X. Jiang, C.Y. Sun, T. Huang, Hypoxia disrupts the expression levels of circadian rhythm genes in hepatocellular carcinoma, *Mol. Med. Rep.* 11 (2015) 4002–4008.
- [36] Z. Chen, L. Liu, Q. Cheng, Y. Li, H. Wu, W. Zhang, Y. Wang, S.A. Sehgal, S. Siraj, X. Wang, J. Wang, Y. Zhu, Q. Chen, Mitochondrial E3 ligase MARCH5 regulates FUNDCl to fine-tune hypoxic mitophagy, *EMBO Rep.* 18 (2017) 495–509.